CFD modelling of a pulsed jet formed during an idealized isolated cough

Marina Zasimova, *Vladimir* Ris, and *Nikolay* Ivanov*

Peter the Great St. Petersburg Polytechnic University, 195251, 29 Politechnicheskaya Str., St. Petersburg, Russian Federation

Abstract. The current contribution presents the results of calculations of a pulsed jet formation during a single cough based on the recent test by Fabregat et al. (2021) where the DNS of an idealized isolated cough was performed. Two approaches for turbulence modeling were applied – the Large Eddy Simulation (LES) and the Unsteady Reynolds-Averaged Navier-Stokes (URANS). The particles propagation was described with the Lagrangian formulation, both with and without interaction with the continuous phase. Unsteady changes in the airflow structure of the pulsed jet are analyzed and discussed, with respect to the accuracy of the turbulence modeling method used. The calculated data show that during the period of 1.5 s the strong pulsed jet dissipates and transforms to a puff. By that instant, the puff front propagates over the distance of up to 0.5 m (URANS data) and 0.6 m (LES data). During the initial period, the URANS data differ from the LES data; nevertheless, at subsequent time instants, the velocity and temperature fields are similar.

1 Introduction

Airborne droplets generated during expiration, cough or sneeze are the main way of the SARS-CoV-2 transmission. The airflow pattern strongly influences the characteristics of droplet transport (e.g., the residence time). The spread of the droplet-borne pathogen along with the exhaled expiratory environment emerged due to expiration, cough or sneeze can be described as a sequence of the following stages:

1. Formation of a turbulent pulsed jet during expiration, cough or sneeze;
2. Jet propagation into the ambient space together with the airborne droplets of various size;
3. Formation of a turbulent cloud carrying pathogenic droplets and its movement with residual inertia;
4. The final stage of the infectious cloud movement up to its dispersion and identity loss in the environment.

To predict pathogen transport and to assess the air quality it is necessary to describe these stages reliably. Air quality assessment could be carried out on the basis of either measurements under model or full-scale conditions (see, e.g., a review of experimental studies in [1]) or Computational Fluid Dynamics (CFD) modelling of 3D turbulent flow and heat and mass transfer using semi-empirical turbulence and multiphase flow models (see, e.g., a review in [2]).

To analyze numerically the droplets transmission mechanisms, and to predict the dangerous cloud of the pathogenic droplets behaviour, it is necessary to reproduce accurately the pulsed jet formation and spreading by means of 3D unsteady computations. As semi-empirical models are widely used for turbulent multiphase flow simulation, the results of computations must be validated with the benchmark experimental or Direct Numerical Simulation (DNS) data. There are few papers presenting results of airborne droplets propagation modelling obtained with high-precision eddy-resolving approaches: Large Eddy Simulation (LES, solution of the filtered Navier-Stokes equations) [3] and DNS [4, 5].

The current contribution presents the results of numerical simulation of a pulsed jet formation during a single cough based on the recent test published by Fabregat et al. in 2021 [4, 5]. In this test the DNS of an idealized isolated cough was performed. The airflow structure forming during a single cough is presented in [4], while the focus of [5] is on the characteristics of droplets propagation. In the present study to simulate the jet formation under conditions [4, 5] two widely used semi-empirical approaches were applied – the Unsteady Reynolds-Averaged Navier-Stokes (URANS) approach coupled with a semi-empirical turbulence model and the LES approach. The particles propagation is described with the Lagrangian formulation.

2 Problem formulation

2.1 Geometry model and boundary conditions

The main part of the computational domain shown in Fig. 1a is a cylinder with the outer diameter of $D = 1$ m and the length of $H = 1.6$ m. Pulsed jet of air with the particles that simulates a single cough is supplied to this space from a small round tube attached to one of the sidewalls of the cylinder. The supply tube has the following dimensions: the diameter of $d = 0.02$ m and the length of $H_p = 0.04$ m (Fig. 2b).

The constant physical properties of air are assumed, namely, density $\rho_a = 1.22$ kg/m^3, dynamic viscosity coefficient $\mu_a = 1.95\times10^{-5}$ kg/m·s, thermal conductivity

Corresponding author: ivanov_ng@spbstu.ru

λ_a = 0.0277 W/m·K, heat capacity $C_{p,a}$ = 1010 J/kg·K, thermal expansion coefficient $\beta_a = 3.36\times10^{-3}$ K^{-1}.

Fig. 1c illustrates the unsteady inlet boundary condition that simulates a single cough. During the coughing process, a spatially uniform air velocity distribution is set at the inlet boundary surface at each time instant. For the first 0.15 s, the air velocity increases linearly from zero to the maximum velocity of $V_{z,max}$ = 4.8 m/s corresponding to the Reynolds number of $Re = \rho d V_{z,max}/\mu = 6\times10^3$. After the instant of 0.15 s with the peak velocity, the inlet velocity started to decrease linearly, and at the instant of 0.4 s the supply flow stops, and the inlet velocity becomes zero again. The supply pipe cylindrical surface as well as the side surface of the cylinder where the supply pipe is attached are the solid walls with the no-slip boundary condition. The uniform gage pressure (an outlet condition) was set at the opposite side surface and the external cylindrical surface.

The ambient air temperature was assumed to be 15°C (it is the initial condition). The constant temperature value of 34°C was set at the inlet to simulate exhaled warm air. The supply pipe wall was assumed as adiabatic.

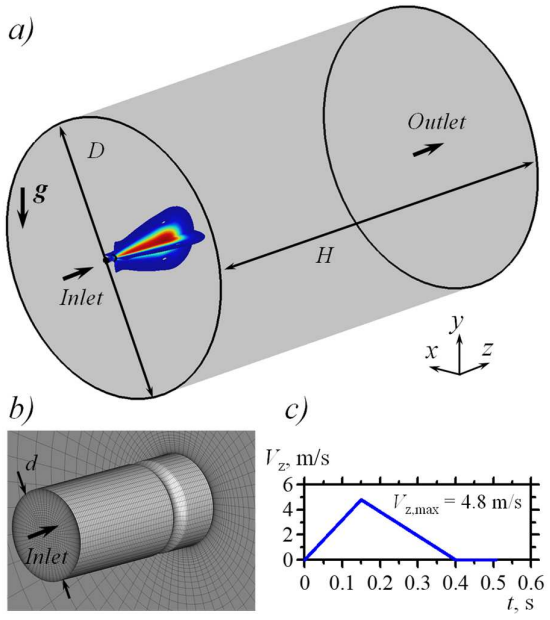

Fig. 1. a) The computational domain and an instantaneous velocity magnitude field obtained in URANS, b) a view of the mesh used for URANS computations near inlet section, c) time evolution of the air velocity at the inlet

According to [5], the particles are assumed as water droplets with the density of ρ_w = 1000 kg/m^3, and heat capacity $C_{p,w}$ = 4180 J/kg·K. The initial velocity of the particles coincides with air velocity at the inlet. Seven different particle diameters d_p of 4, 8, 16, 32, 64, 128 and 256 μm, are considered. The characteristic time of the particles, $t_0 = \rho_w d_p^2/18\mu_a$, is in the range of 4.6×10^{-5}…0.19 s. The values of the Stokes number calculated using the supply tube diameter, d, and the mean velocity (averaged over one cough release), $V_{z,max}/2$, is less than 1 for cases with the particle diameters d_p < 32 μm and more than 1 for d_p > 64 μm.

The particles are released from the inlet section at 69 points locations (the locations used in the current study coincide with the locations denoted in [5]). The duration of particle release is 0.4 s, the total amount of particles of each particular diameter is 13 800. It is assumed that the particles leave the computational domain through the outlet boundaries, and the escape boundary condition is set there.

2.2 Mathematical model and numerical aspects

Two approaches were used for turbulent airflow (the continuous phase) modelling: the eddy-resolving LES approach and the URANS approach combined with a semi-empirical turbulence model: k-ε RNG or k-ω SST model (a special study of the turbulence model influence on the solution was performed). The following inlet turbulence characteristics were used: the turbulence intensity I = 5 % and the turbulent viscosity ratio TVR = 10. For the continuous phase, the buoyancy effects were taken into account using the Boussinesq approximation. The dynamics of the droplet propagation (the discrete phase) was modelled based on the Lagrangian approach. To investigate the effects of the influence of particles on the airflow, two approaches were used for discrete phase modelling: with and without interaction with the continuous phase. For the URANS calculations, a special study of the turbulent dispersion influence on the particle transport simulation was performed: the computations were performed for the cases with and without turbulent dispersion model. Discrete random walk model was used to model the turbulent dispersion with the time scale constant 0…0.1.

The computational grids were generated with ICEM CFD. The URANS calculations used a grid consisted of hexagonal cells with the total size 0.6 million cells (see Fig. 1b). The LES calculations used a uniform grid consisted of identical polyhedral cells in the outer region and prismatic layers near solid boundaries, the total grid size was about 35 million cells.

Numerical solutions were obtained with the CFD package ANSYS Fluent based on the finite volume method with the cell-centered variable arrangement. The time step value was 0.0005 s for all the cases considered. The second order temporal and spatial schemes were activated. The calculations used the resources of Super Computer Center (SCC) «Polytechnic» (www.scc.spbstu.ru). The cases obtained with the LES approach used 512 cores, URANS – 26.

3 Results and discussions

3.1 Airflow pattern

The cough in the present study was modelled as a pulsed jet generated during the period of 0.4 s; during the initial 0.15 s a rapid increase of the flow rate and momentum occurs. A stable (almost laminar) airflow with the ring-shape structure is formed during this period. Fig. 2 presents instantaneous velocity and temperature fields at the middle plane x = 0 for the time instant of t = 0.15 s (the peak of inlet velocity); both the LES and URANS

(with k-ε RNG turbulence model) data are illustrated. The ring-shape structure is visible at $z > 0.1$ m (Fig. 2), and both the LES and URANS models qualitatively predict it. However, even during the initial stage of the pulse jet formation ($t < 0.2$ s) there is noticeable difference between the LES and URANS results. The LES results demonstrate sharper field distribution as compared with the URANS data; LES data are in better agreement with the DNS data described in [4, 5].

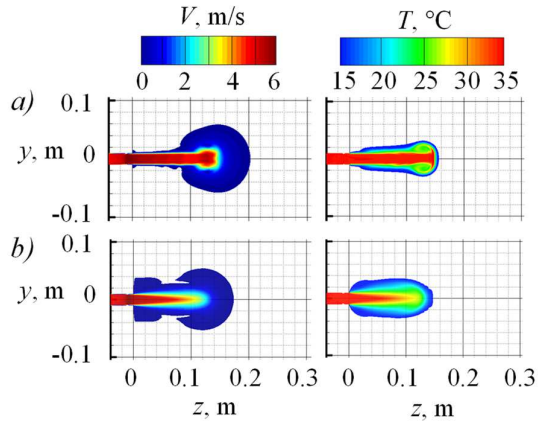

Fig. 2. The velocity and temperature fields at time instant $t = 0.15$ s obtained in a) LES and b) URANS (with k-ε RNG model) calculations (for the cases without particle release)

The calculated data show that the strong pulsed jet dissipates during the period of 1.5 s or even longer. Fig. 3 illustrates time-evolution of the air movement generated by the pulsed jet after the cough is over. Velocity fields at the middle plane are given in the figure for both LES and URANS cases. It is evident that a thermal puff is formed. Analysis of the thermal puff behaviour could be found, e.g., in [6, 7].

The thermal puff has relatively small velocity values, but it is clearly determined in all plots in Fig. 3, and it is supposed to lose its identity later, when it fully dissipates in the environment. For the computed period of 1.5 s, the jet front propagates over the distance of up to 0.5 m (URANS data) and 0.6 m (LES data). At subsequent time instants ($t > 0.4$ s), the velocity and temperature fields in the LES and URANS look different. Note that the change of the turbulence model in URANS simulation do not change the velocity and temperature fields much.

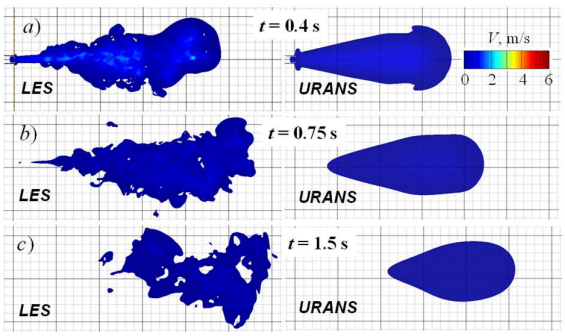

Fig. 3. The evolution of velocity fields obtained in LES and URANS (with k-ε RNG model) calculations (for the cases without particle release)

3.2 Particles transport

Fig. 4 demonstrates time evolution of particle positions during an isolated cough computed with the LES approach, while Fig. 5 illustrates the same data obtained with the URANS approach. It is evident from both the sets of the plots, that during the pulse jet formation and spreading, particles with different mass (diameter) have strongly different trajectories.

According to the literature (see, for example, the experimental studies of scientific group from MIT, http://lbourouiba.mit.edu/), during the cough large «ballistic» droplets with diameters more than 200 µm settle at distances not exceeding 0.6 m from the source of pollution, and they serve as the main source of contamination of solid surfaces.

In the present study, it is shown that in both the LES and URANS results by the instant of 0.4 s the distance from the source of particle release to the extreme particles that move from the inlet with the peak velocity values does not exceed 0.6 m. The heavy particles with large diameters – 64 µm and more (or with the Stokes number exceeding the value of 1) movement is preconditioned by the initial momentum. Fig. 4, 5 show that for these particles the trajectories obtained with different turbulence modelling approach (LES or URANS with different turbulence models) are almost similar. The only difference in the results is in local characteristics: the LES-obtained trajectories (Fig. 4) look more chaotic in comparison with the URANS data (Fig. 5). If a discrete random model is used to model turbulent dispersion in URANS calculations, the local particle positions look more like LES data, but it does not change the mean values of locations.

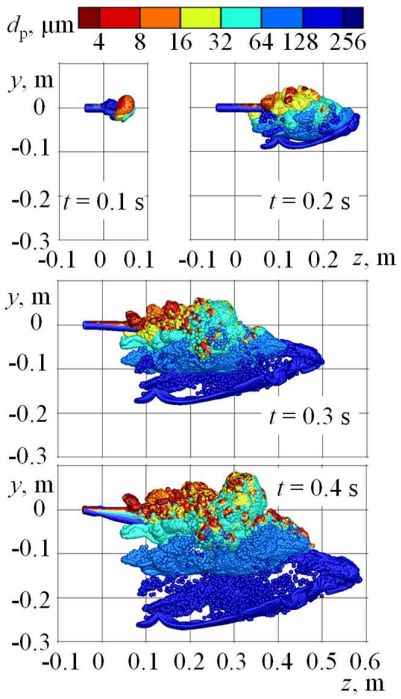

Fig. 4. The evolution of particles locations obtained in LES calculations (case with interaction with a continuous phase); particles are coloured by the diameter

The trajectories of the relatively light particles with small diameter values – 32 µm and less (or with the Stokes number less than 1) are in accordance with the airflow pattern. Therefore, the effect of the turbulence model used (e.g., LES or URANS) on the trajectories of particles with small diameters is significant (Fig. 4, 5), especially for the time period $t \geq 0.2$ s.

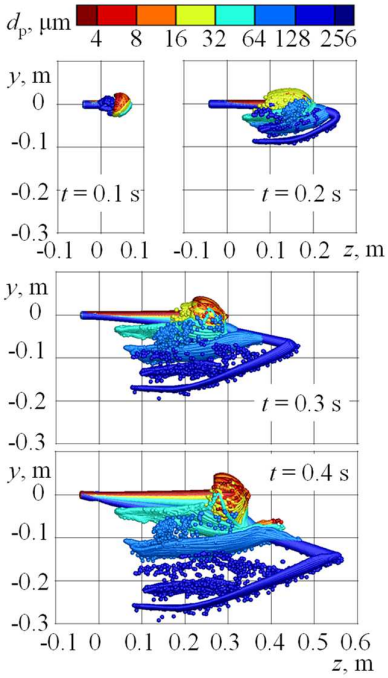

Fig. 5. The evolution of particles locations obtained in URANS (with *k-ε* RNG model) calculations (case with interaction with a continuous phase); particles are coloured by the diameter

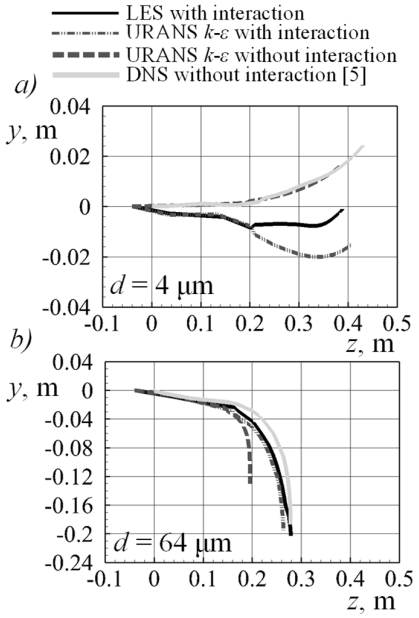

Fig. 6. The puff center evolution for the particles with diameter a) 4 µm and b) 64 µm obtained in LES and URANS (with *k-ε* RNG model) calculations

The puff generated from the pulse jet by the instant of 0.4 s is clearly observed both in Fig. 3 (velocity field) and in Fig. 4, 5 (particle cloud). Thus, by the end of the cough the light particles are collected in a cloud (or the puff).

To characterize the puff position quantitatively, the coordinates of its center were estimated for all the cases considered. The puff center (*y* and *z* coordinates) for the particles with the same diameters at the fixed time instants were computed. Fig. 6 shows the puff center time evolution both for small (light) particles with diameter of 4 µm (Fig. 6a) and for large (heavy) particles with diameter of 64 µm (Fig. 6b). Data computed with the LES and URANS approached are compared with the DNS data from [5].

The results of the present calculations are shown for cases with and without particles interaction with a continuous phase. It is evident that the LES and URANS results do not differ much. For the case without particles interaction with a continuous phase, a satisfactory agreement with DNS data [5] is observed for small particles, Fig. 6a. The influence of the particle interaction modeling is pronounced, especially for the particles with large diameter (64 µm and more).

4 Conclusion

Results of LES and URANS calculations of a pulsed jet formation during a single cough based on the recent test by Fabregat et al. (2021) show that during the period of 1.5 s the strong pulsed jet dissipates and transforms into a clearly identified puff. By the instant of 1.5 s, the puff front propagates over the distance of up to 0.5 m (URANS data) and 0.6 m (LES data). During the initial period (at t < 0.2 s), the URANS data differ significantly from the LES data; nevertheless, at subsequent time instants, both the approaches give similar results. By the end of the cough, the puff collects light particles.

The study was supported by the Russian Science Foundation, grant no. 22-79-10104

References

1. Y. Li, G. M. Leung, J.W. Tang, X. Yang, C.Y.H. Chao, J.Z. Lin, J. W. Lu, P. V. Nielsen, J. Niu, H. Qian, A.C. Sleigh, H.-J. J. Su, J. Sundell, T. W. Wong, P.L. Yuen, Indoor Air **17**, 2 (2007)
2. S. Peng, Q. Chen, E. Liu, Science of the Total Environment **746**, 142090 (2020)
3. D. Fontes, J. Reyes, K. Ahmed, M. Kinzel, Physics of Fluids **32**, 111904 (2020)
4. A. Fabregat, F. Gisbert, A. Vernet, S. Dutta, K. Mittal, J. Pallares, Physics of Fluids **33**, 035122 (2021)
5. A. Fabregat, F. Gisbert, A. Vernet, J.A. Ferre, K. Mittal, S. Dutta, J. Pallares, Physics of Fluids **33**, 033329 (2021)
6. E. Ghaem-Maghami, H. Johari, Journal of Fluids Engineering **129**, 194 (2007)
7. E. Ghaem-Maghami, H. Johari, Physics of Fluids **22**, 115105 (2010)